中國海洋大學

NUMERICAL ANALYSIS ON THE REFLECTION COEFFICIENT OF A CURTAIN BREAKWATER USING OPENFOAM

Shengqiang Yin, Xinyu Wang, Yong Liu

Shandong Provincial Key Laboratory of Ocean Engineering, Ocean University of China, Qingdao, Shandong Province, China

2018.06.26

Contents

Brief introduction

The curtain breakwater, as a new type of breakwater, is developed from vertical plate-type breakwaters.Compared with traditional caissons breakwaters, it has a great advantage:

- The incident wave energy is dissipated by the vortex flows around the drooping plate effectively, and thus has a lower reflection coefficient.

Research on the hydrodynamic performance of curtain breakwaters has been of great interest since the last century. Very important developments have been achieved thanks to the efforts of different researchers.

- Nakamura et al. (1999) experimentally studied the hydrodynamic performance of a curtain breakwater and analyzed the effects of the chamber width and the immersed depth of the drooping plate on the reflection coefficient of the breakwater.
- Ono et al. (2003) analyzed the flow field around a vertical plate.

Brief introduction

My study presents a two-dimensional numerical investigation on the reflection coefficient of **a curtain breakwater** including a seaside drooping plate and a leeside caisson. The variations of the reflection coefficient versus factors of **the wavelength**, **the wave chamber width**, **the immersed depth of the drooping plate** and **the angle at the bottom of the drooping plate** are examined.

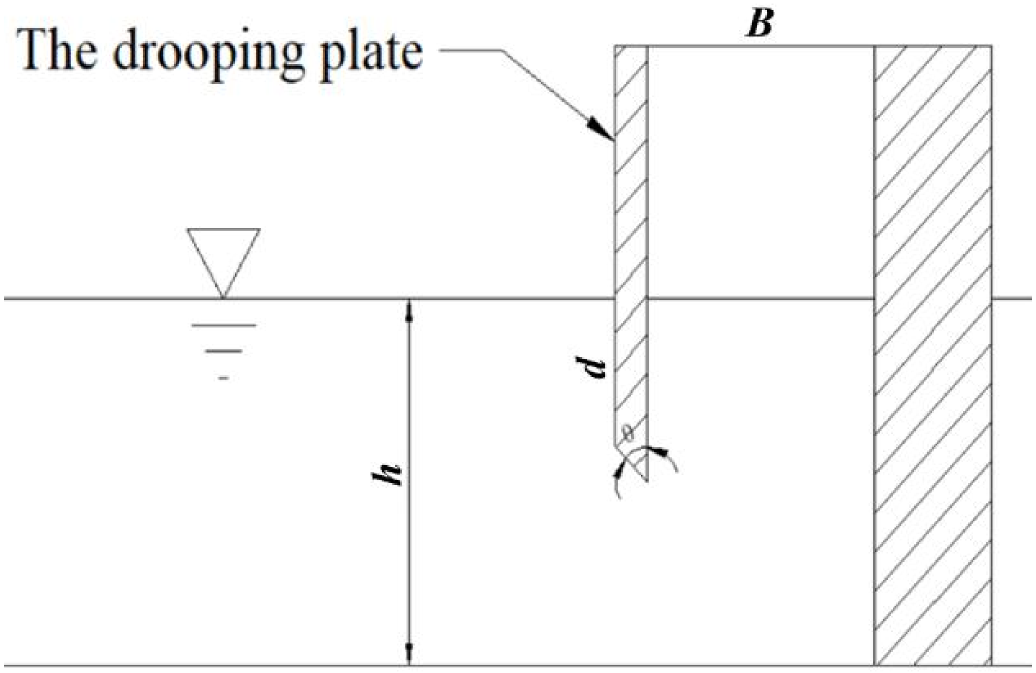

Figure 1 Sketch of a curtain breakwater

Numerical methods

➢ Governing equations

In this study, both air and water are **incompressible viscous fluid**. The continuity equation and momentum equation for incompressible viscous fluid are expressed as below:

Continuity equation:

$$\frac{\partial u}{\partial x}+\frac{\partial v}{\partial y}=0$$

Momentum equation

$$\frac{\partial u}{\partial t}+u\frac{\partial u}{\partial x}+v\frac{\partial u}{\partial y}=-\frac{1}{\rho}\frac{\partial p}{\partial x}+\frac{\mu}{\rho}(\frac{\partial^2 u}{\partial x^2}+\frac{\partial^2 u}{\partial y^2})$$

$$\frac{\partial v}{\partial t}+u\frac{\partial v}{\partial x}+v\frac{\partial v}{\partial y}=-\frac{1}{\rho}\frac{\partial p}{\partial y}+\frac{\mu}{\rho}(\frac{\partial^2 v}{\partial x^2}+\frac{\partial^2 v}{\partial y^2})+g$$

Numerical methods

➢ VOF

The phase fraction *α* is used to represent the volume fraction of the water in each cell:

α=0.5

$$\begin{cases} \alpha = 0 & \text{air} \\ 0 < \alpha < 1 & \text{the free surface} \\ \alpha = 1 & \text{water} \end{cases}$$

The phase fraction equation is given by:

$$\frac{\partial \alpha}{\partial t} + \nabla \cdot (\alpha \mathbf{U}) + \nabla \cdot [\alpha(1-\alpha)\mathbf{U}_r] = 0$$

Ur is the relative velocity of liquid and gas. The density and viscosity of each cell can be calculated by:

$$\rho = \alpha_{water}\rho_{water} + (1 - \alpha_{water})\rho_{air}$$

$$\mu = \alpha_{water}\mu_{water} + (1 - \alpha_{water})\mu_{air}$$

Numerical methods

➢ Wave theory

The second-order Stokes wave theory is adopted. The surface elevations and velocity of second-order Stokes wave are given by the following equations.

$$\eta = \frac{H}{2}\cos(kx-\omega t)+\frac{1}{4}\left(\frac{H}{2}\right)^{2}k\cos 2(kx-\omega t)$$

$$\begin{cases} u = \frac{H\omega}{2}\left(\frac{\cosh k(y+h)}{\sinh kh}\cos(kx-\omega t)+\frac{3}{4}\frac{H}{2}k\frac{\cosh 2k(y+h)}{\sinh^{4}kh}\cos 2(kx-\omega t)\right) \\ \\ v = \frac{H\omega}{2}\left(\frac{\sinh k(y+h)}{\sinh kh}\sin(kx-\omega t)+\frac{3}{4}\frac{H}{2}k\frac{\sinh 2k(y+h)}{\sinh^{4}kh}\sin 2(kx-\omega t)\right) \end{cases}$$

Verification of numerical results

Ocean University of China

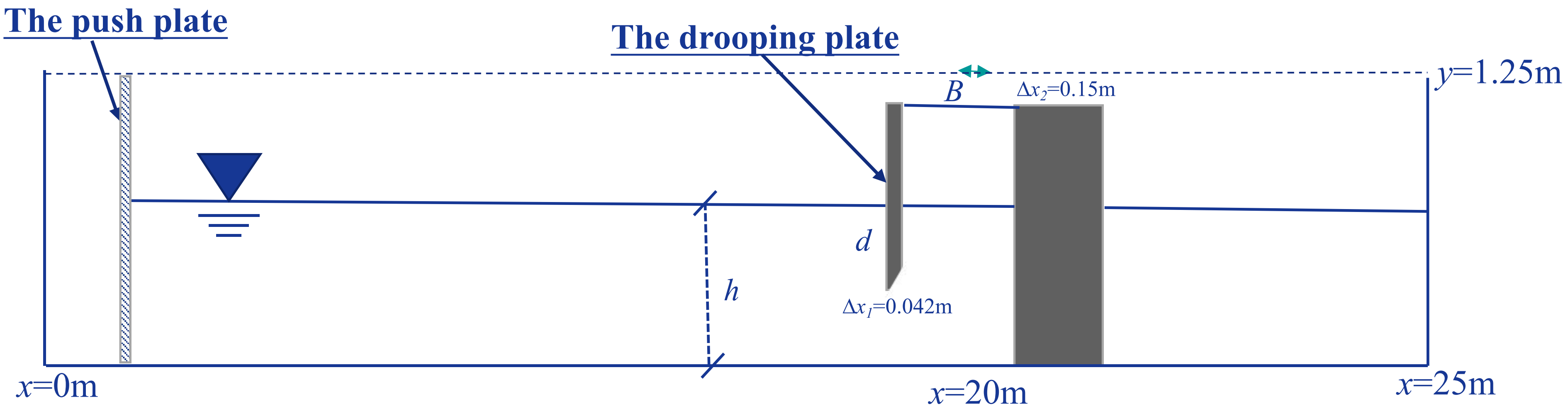

Figure 2 The experimental wave flume

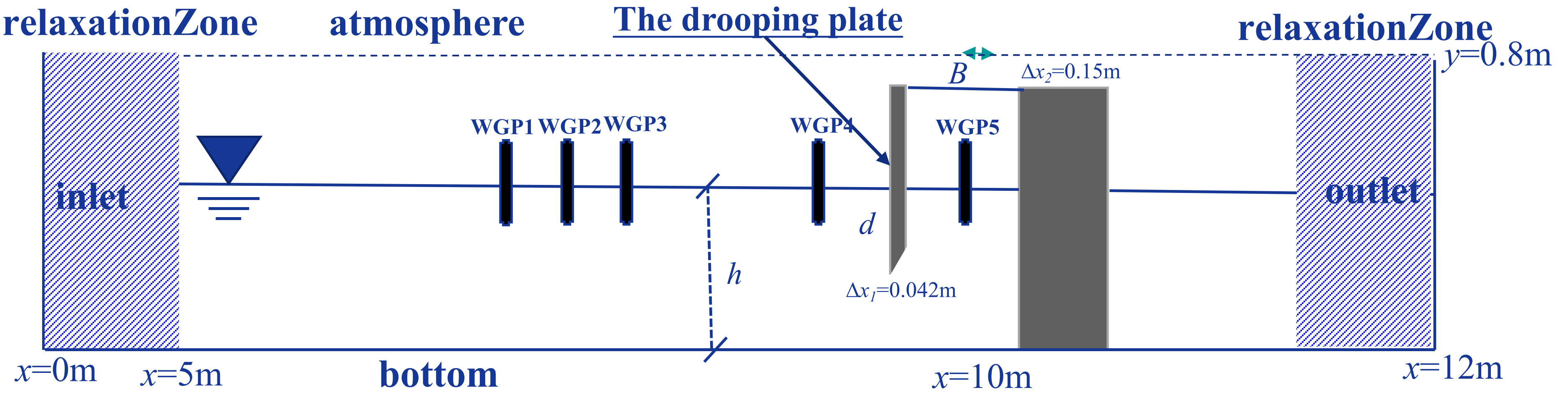

Figure 3 The numerical wave flume

Verification of numerical results

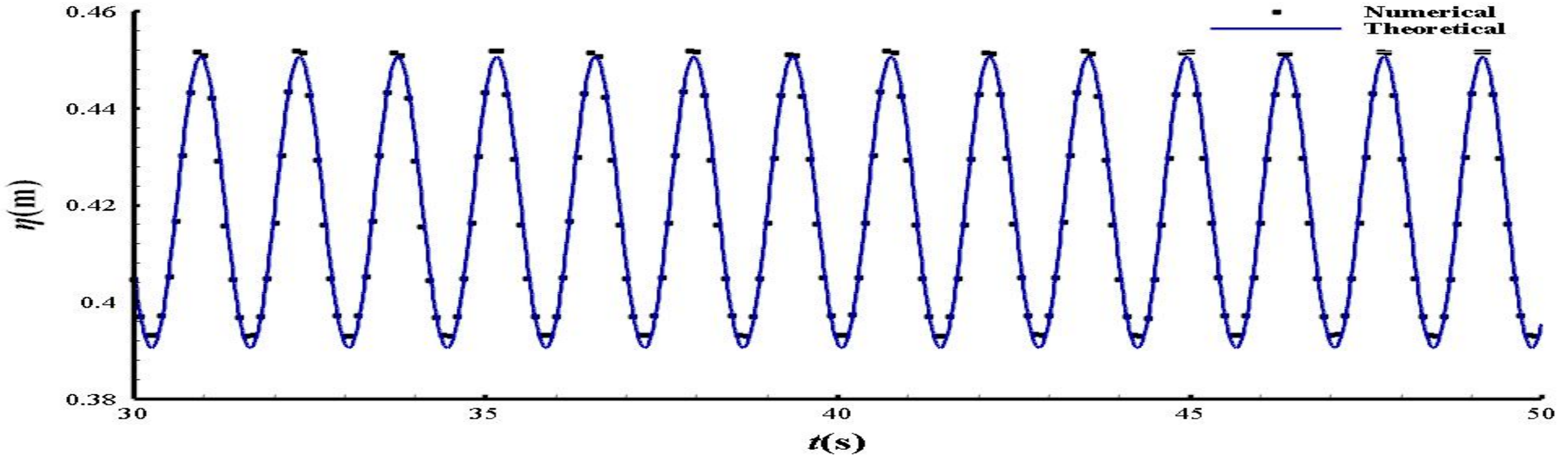

Figure 4 Free surface elevations at x=10 m without breakwaters of second-order Stokes waves（*T*=1.4s）

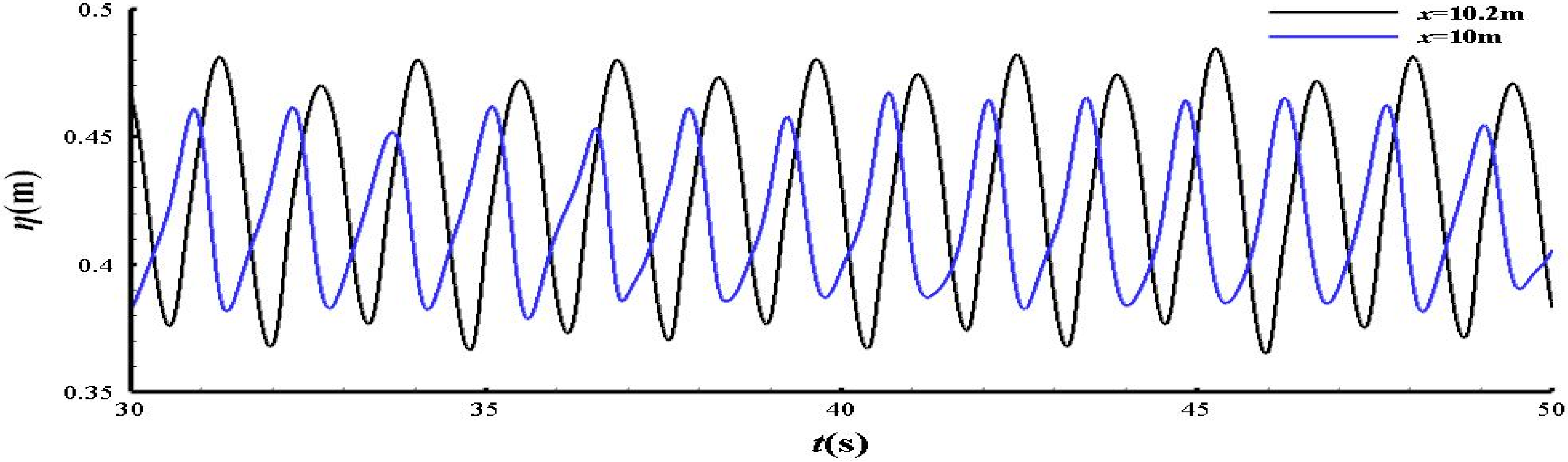

Figure 5 Wave surface elevations at different locations with breakwaters （*T*=1.4s）

Verification of numerical results

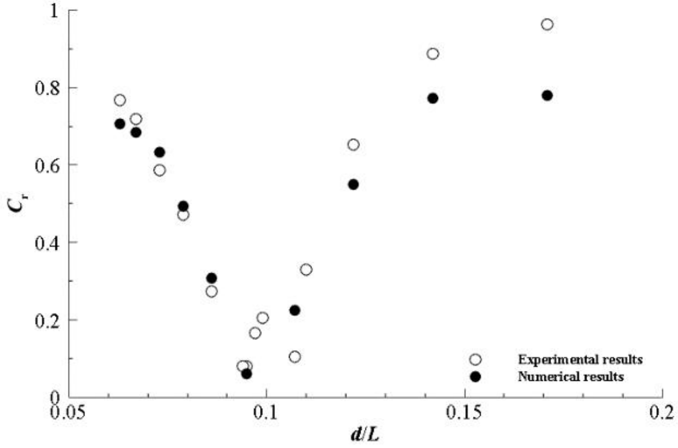

Figure 6 Variation of C_r versus d/L (B=21 cm, d=21 cm, θ=45°)

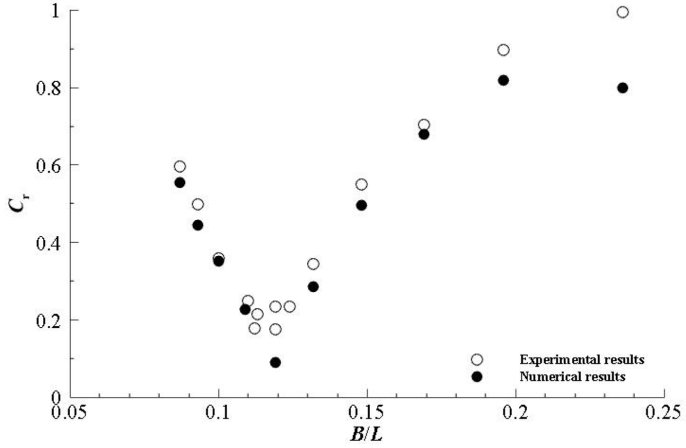

Figure 7 Variation of C_r versus B/L (B=29 cm, d=21 cm, θ=45°)

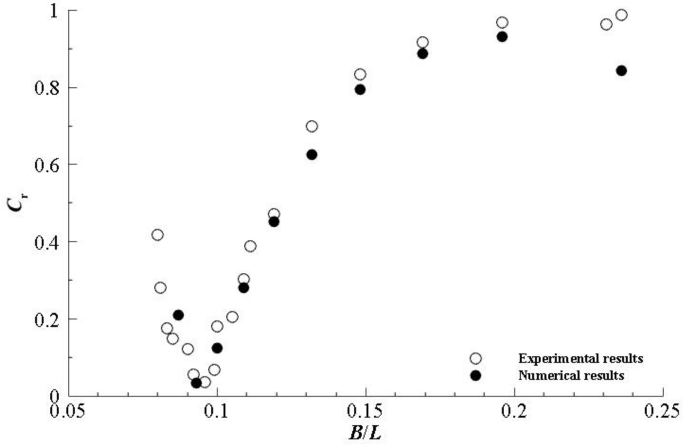

Figure 8 Variation of C_r versus B/L(B=29 cm,d=29 cm,θ=45°)

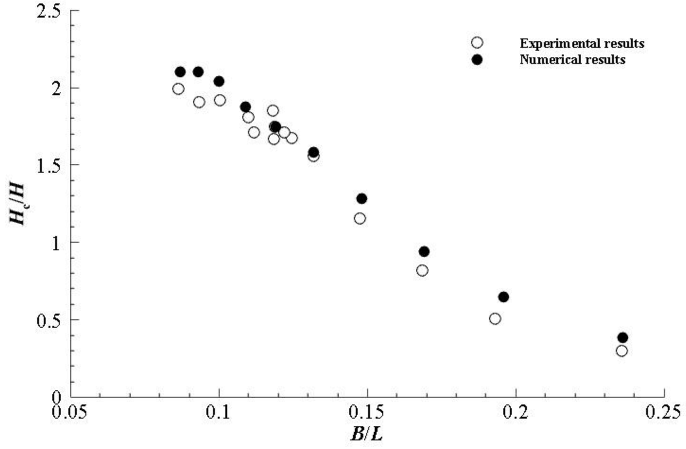

Figure 9 Variation of H_c/H versus B/L(B=29 cm,d=21 cm, θ=45°)

The numerical results of the reflection coefficient C_r and the free surface elevation H_c inside the wave chamber are compared with the experimental data of Nakamura et al. (1999).

Further discussions

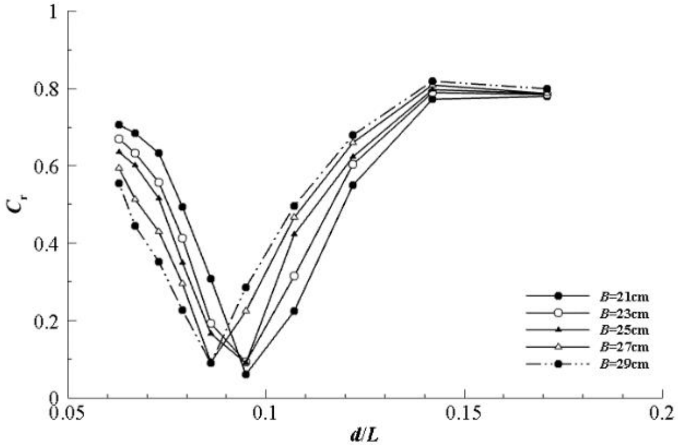

Figure 10 Variation of C_r versus d/L（d=21 cm, θ=45°）

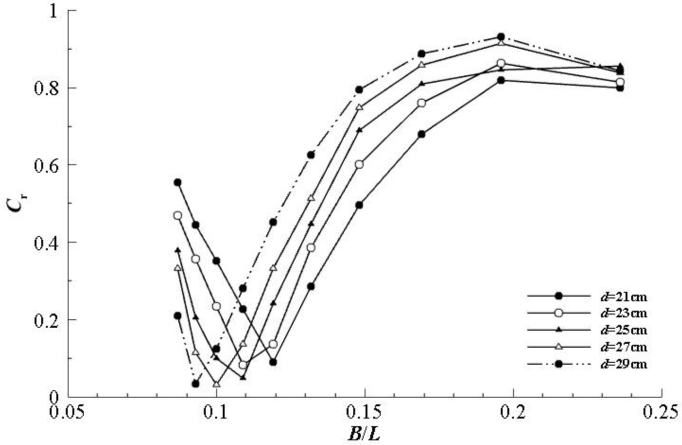

Figure 11 Variation of C_r versus B/L（B=29 cm, θ=45°）

For reaching lower reflection, the values of the wave chamber width should be around one tenth of the wavelength.

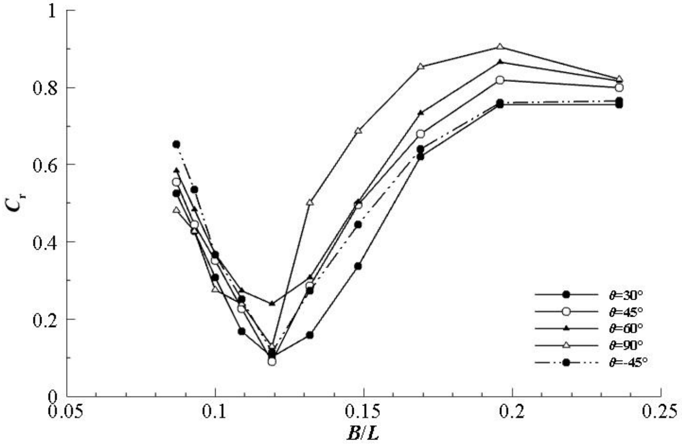

Figure 12 Variation of C_r versus B/L(B=29 cm, d=21 cm)

It is noted from this figure that the reflection coefficients of curtain breakwater at positive and negative angles are close. The drooping plate with a shaper corner generally can dissipate more incident wave energy.

Further discussions

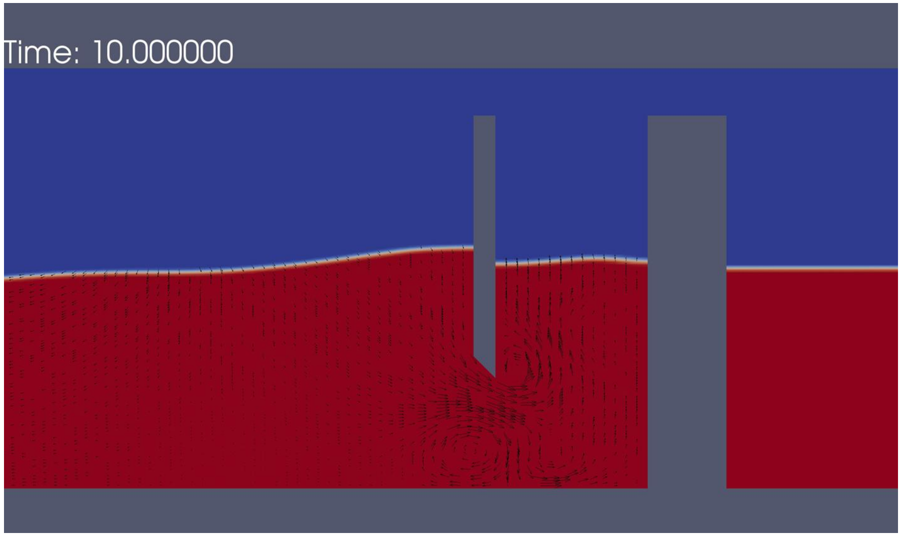

Figure 13 The free surface around the drooping plate

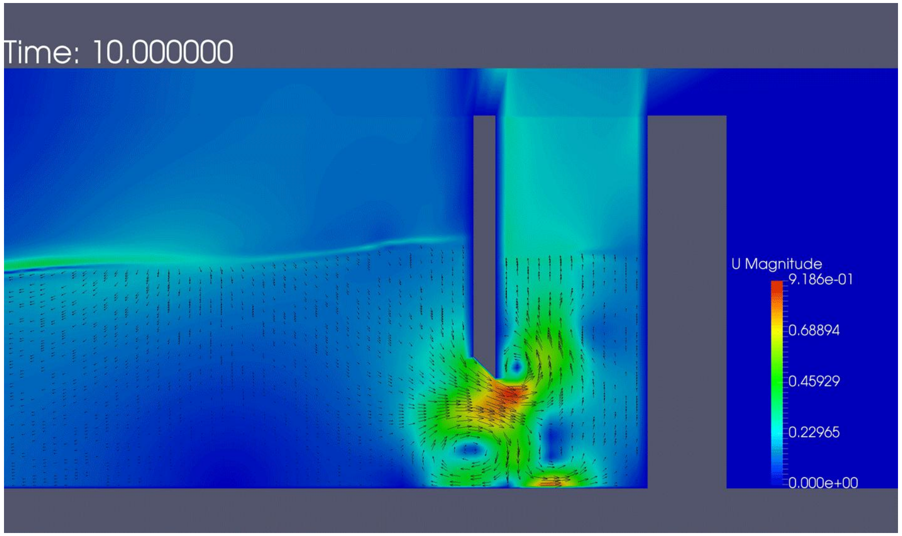

Figure 14 The flow fields around the drooping plate

In these figure, vortex flows at the bottom of the drooping plate can be clearly observed, and the incident wave energy is dissipated by the vortex flows effectively.

Conclusion

- The numerical results of the reflection coefficient and the free surface elevation inside the wave chamber of the curtain breakwater are in a good agreement with the experimental data in literature. The present numerical solution based on OpenFOAM can well simulate the hydrodynamic performance of the curtain breakwater.

- For reaching a low reflection coefficient, the wave chamber width of the curtain breakwater should be designed as about one tenth of the incident wavelength.

- The positive and negative sloping angles at the drooping plate bottom cannot bring significant difference on dissipating incident wave energy.

- The irregular wave action on the curtain breakwater will be examined in the next study.

中國海洋大學

Thank you !